Tellus (1985), *37A*, 87–96

On the diffusive salt flux of the Baltic proper

By LARS RAHM, *Department of Oceanography, University of Gothenburg, Box 4038, S-400 40 Gothenburg, Sweden*

(Manuscript received April 11; in final form June 27, 1984)

ABSTRACT

Turbulent cross-isohaline salt fluxes in the Baltic proper are studied with the aid of a one-dimensional "advection-diffusion" model. The theoretical framework of this model has been outlined by Walin. It is based on time-averaged T–S data from both the inflow and interior regions of the Baltic. The results obtained are in good agreement with some estimates of the mixing properties in the region. Based on this investigation, a discussion of the properties of the model and its applicability to a real estuarine system is performed.

1. Introduction

It is a long-felt wish to be able to gain some information from the vast amount of hydrographic data (though of varying quality) that has been collected from the Baltic during the last century, especially in light of the changes of state that have occurred. This is a result of a complicated interplay between certain hydrographic conditions, the supply of certain chemical substances and biological activity. Consider e.g., the decreasing oxygen concentration and the increasing tendencies of eutrophication in the Baltic Sea during this century. An appropriate quantitative description of the general circulation in this area is a prerequisite for an understanding of the underlying mechanisms causing these changes.

The circulation picture we have of the Baltic proper today has been built up by a variety of means and data. Large-scale property distributions such as salinity and temperature have played an important rôle in inferences on the large-scale time-averaged movements of the water. This is due to the fact that the property distributions are a more convincing basis on which to build a picture of the mean circulation than most other methods.

Box models (see e.g. Bolin, 1972), in one form or another, have been used for this purpose. These models require, however, a drastic reduction of the continuous property fields to only a few carefully selected points. Thus the resolution by necessity becomes rather crude. The utilization of "diagnostic" models similar to those used in the context of ocean circulation (see e.g. Holland (1971) or, in the context of the Baltic, Sarkisyan et al. (1978)) would drastically improve the resolution, though their complexity hampers their use. Further, experience shows that requirements on the data sets used are considerable. For a critical review of the various "diagnostic" models, see Veronis (1975).

An intermediate "route" has been suggested by Walin (1977), who derived the theoretical framework for a simple diagnostic model potentially suitable for estuaries like the Baltic. It is a one-dimensional "advection-diffusion" model with salinity as a space-variable. This choice of variable is motivated by the fact that the density variation in the deeper parts of the Baltic is dominated by the salt concentration. As in both box and "diagnostic" models, real observed hydrographic data (though generally smoothed and averaged in some way) are substituted into the governing equation, whereupon the sought property distribution is calculated.

The purpose of this work is to determine the turbulent salt flux of the Baltic proper by using Walin's model and already existing hydrographic data. The latter is economically very attractive as generation of new data is rather expensive. This is done as a case study in order to investigate the characteristic features of the model and its applicability to a real estuarine system.

A more "direct route" is also outlined in Walin's (1977) work. This method is based solely on direct measurements of the inflow characteristics of the actual basin, but its applicability is unfortunately hampered by the scarcity of suitable data, though considerable efforts have recently been made to improve this situation (see Rydberg, 1978; Walin, 1981). In a study of the denitrification process in the Baltic (Shaffer and Rönner, 1984) this "direct route" has been used to estimate the mean turbulence field. Despite the lack of data, a comparison between the results from these two "routes" is carried out in this paper.

The outline of the paper is as follows. The governing equation and its boundary conditions are given in Section 2, whereafter the actual estuarine system and its hydrographic data are presented in Section 3 together with the analytical solution obtained. In Section 4 a discussion of the various implications of the resulting solutions is given.

2. Theoretical background

The following calculations are, as mentioned above, based on a theoretical study by Walin (1977) and therefore only the main features of his theory will be outlined below. The continuous functions describing the state of a semi-enclosed system are, in his model, solely dependent on salinity S and time t. The variation of other constituents is assumed to be small along the isohalines.

2.1. The model equations

Conservation of volume applied to the region of interest below an isohaline surface S' implies (see definition sketch, Fig. 1):

$$\frac{\mathrm{d}}{\mathrm{d}t} V(S', t) = M(S', t) - G(S', t), \tag{2.1}$$

where $V(S', t)$ is the total volume below the isohaline S' and $M(S', t)$ is the net supply of fluid to the region in the salinity range $S \geqslant S'$. Finally, $G(S', t)$ represents the volume flux through the S'-isohaline surface. The conservation of salt content J below this surface is thus dependent on three terms: the inflow M, the cross-isohaline advective

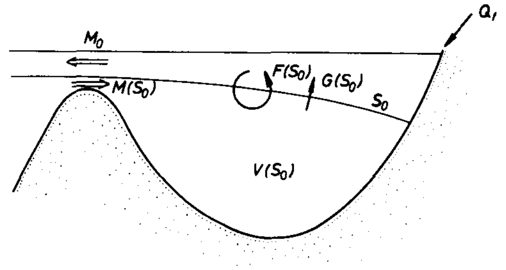

Fig. 1. Definition sketch showing the physical model. It represents an estuary wherein the isohaline surface S_0 separates the brackish "homohaline" surface layer from the stratified deeper parts of the basin of volume $V(S_0)$. Q_f and M_0 are the freshwater supply and the surface water discharge, respectively. The net deep-water inflow $M(S_0)$ and the corresponding salt-transport reaches the surface layer by the advective flow $G(S_0)$ and the turbulent flux $F(S_0)$.

flux G and the diffusive salt flux F. This can be expressed as

$$\frac{\mathrm{d}J}{\mathrm{d}t} = -G \cdot S + \int_{S'}^{\infty} m \cdot S \,\mathrm{d}S - F, \tag{2.2}$$

where

$$\frac{\mathrm{d}M}{\mathrm{d}S} = -m(S', t), \tag{2.3}$$

$$\frac{\mathrm{d}V}{\mathrm{d}S} = -\vartheta(S', t). \tag{2.4}$$

Here $m\,\mathrm{d}S$ and $v\,\mathrm{d}S$ represent the inflow and volume of fluid in the salinity range $S' \leqslant S \leqslant S' + \mathrm{d}S$. Eqs. (2.1) and (2.2) yield (*cf.* Walin, 1977)

$$\frac{\mathrm{d}F}{\mathrm{d}S} = -G, \tag{2.5}$$

or combined with (2.2)

$$\frac{\mathrm{d}V}{\mathrm{d}t} = M + \frac{\mathrm{d}F}{\mathrm{d}S} \tag{2.6}$$

This equation offers in steady-state, as mentioned in Section 1, a straightforward way to estimate the overall mixing properties of the basin by direct observations of only the inflow characteristics.

One is also able to determine $F(S', t)$ in an "indirect" way by assuming that some other "substance" is mixed by the same turbulence field as salt. Temperature will be used as such a "substance" in the following calculations and further, it can be treated as a conservative tracer in the deeper parts of the Baltic. The governing equation for the diffusive flux F is obtained in an analogous way to eq. (2.2). It becomes (*cf.* Walin, 1977) in steady-state form;

$$(\gamma - T)\frac{d^2F}{dS^2} + \frac{d^2T}{dS^2}\cdot F = 0, \qquad (2.7)$$

where $T(S, t)$ is a weighted mean temperature over the isohaline surface S in the basin and $\gamma(S, t)$ is the corresponding mean temperature of the inflowing water.

2.2. *The boundary conditions*

The applicability of eq. (2.7) is limited to the stratified part of the basin as the relation between T and S is non-unique in the brackish surface layer. Let us assume that the latter layer has a mean salinity S_0 and that eq. (2.7) is defined in the interval $S_0 \leqslant S \leqslant S_{max}$, where S_0 and S_{max} are the salinity at the top of the halocline (equal to that of the surface layer) and the maximum observed salinity at the bottom of the basin, respectively. Further, we assume steady-state conditions.

As there is no turbulent salt flux through the bottom, the corresponding boundary condition becomes

$$F = 0, \quad \text{at} \quad S = S_{max}. \qquad (2.8)$$

This implies that either F has an inflexion point or $\gamma = T$ at the bottom, i.e. M either vanishes or is finite at the maximum salinity.

The second boundary condition is obtained by matching the turbulent flux at the top of the halocline with that of the surface brackish layer. The latter is determined to "lowest order" by the "Knudsen relations" (see also Fig. 1). Volume and salt continuity yield

$$\int_{S_0}^{S_{max}} m\,dS + Q_f = M_0, \qquad (2.9)$$

$$\int_{S_0}^{S_{max}} m\cdot S\,dS = M_0\cdot S_0, \qquad (2.10)$$

where Q_f and M_0 are the freshwater supply and surface water discharge, respectively. Note that the precipitation and the evaporation equal each other in the Baltic Sea. Continuity in salt flux to or from the deeper parts of the basin yields

$$\int_{S_0}^{S_{max}} m\cdot S\,dS = S_0\cdot G(S_0) + F(S_0), \qquad (2.11)$$

or, by utilizing (2.1, in steady state), (2.9) and (2.10), the sought boundary condition becomes

$$F(S_0) = Q_f\cdot S_0. \qquad (2.12)$$

3. Calculations

The model is applied to the Baltic proper, which represents an overmixed estuary in that the semi-enclosed basin has a halocline well below its entrance to the Kattegat. This halocline separates the brackish, "homohaline", surface layer from the stratified deeper parts. The Baltic will, for convenience, be divided into two regions. One, the inflow region, represents the southern part of the Baltic from the Bornholm Strait to the eastern end of the Stolpe Channel. In this region, water is entrained from the surface layer to the underlying "deep" water. The other region consists of the deeper parts of the Baltic where the inflowing water spreads out and, one way or another, returns to the Kattegat via the surface layer. This region is composed of the Eastern Gotland and Fårö Basins, the Northern Central Basin and the Landsort and Western Gotland Basins (see Fig. 2).

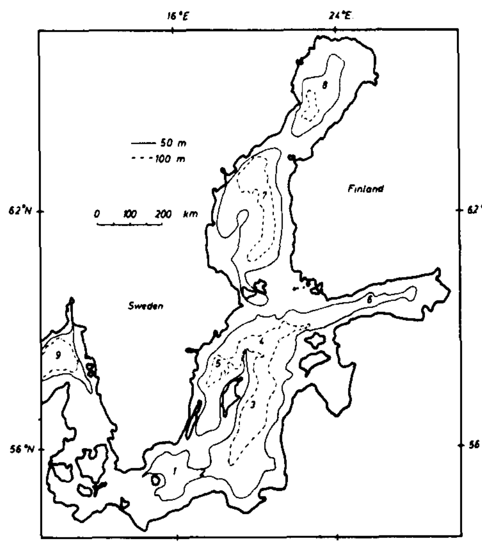

Fig. 2. Index map identifying the different basins in the Baltic Sea including an approximative representation of the 50 m and 100 m isobaths. The different areas are as follows: Bornholm Basin (1), Stolpe Channel (2), Eastern Gotland and Fårö Basins (3), Northern Central Basin (4), Landsort and Western Gotland Basins (5), Finnish Gulf (6), Bothnian Sea (7), Bothnian Gulf (8) and Skagerrak (9).

3.1. The hydrographic data

One hydrographic station, BY15, situated in the Eastern Gotland Basin, has been chosen as the sole representative for the entire interior region. This assumption is to some extent justified by the high degree of lateral homogeneity observed in the Baltic. Only small differences are found, as is evident in

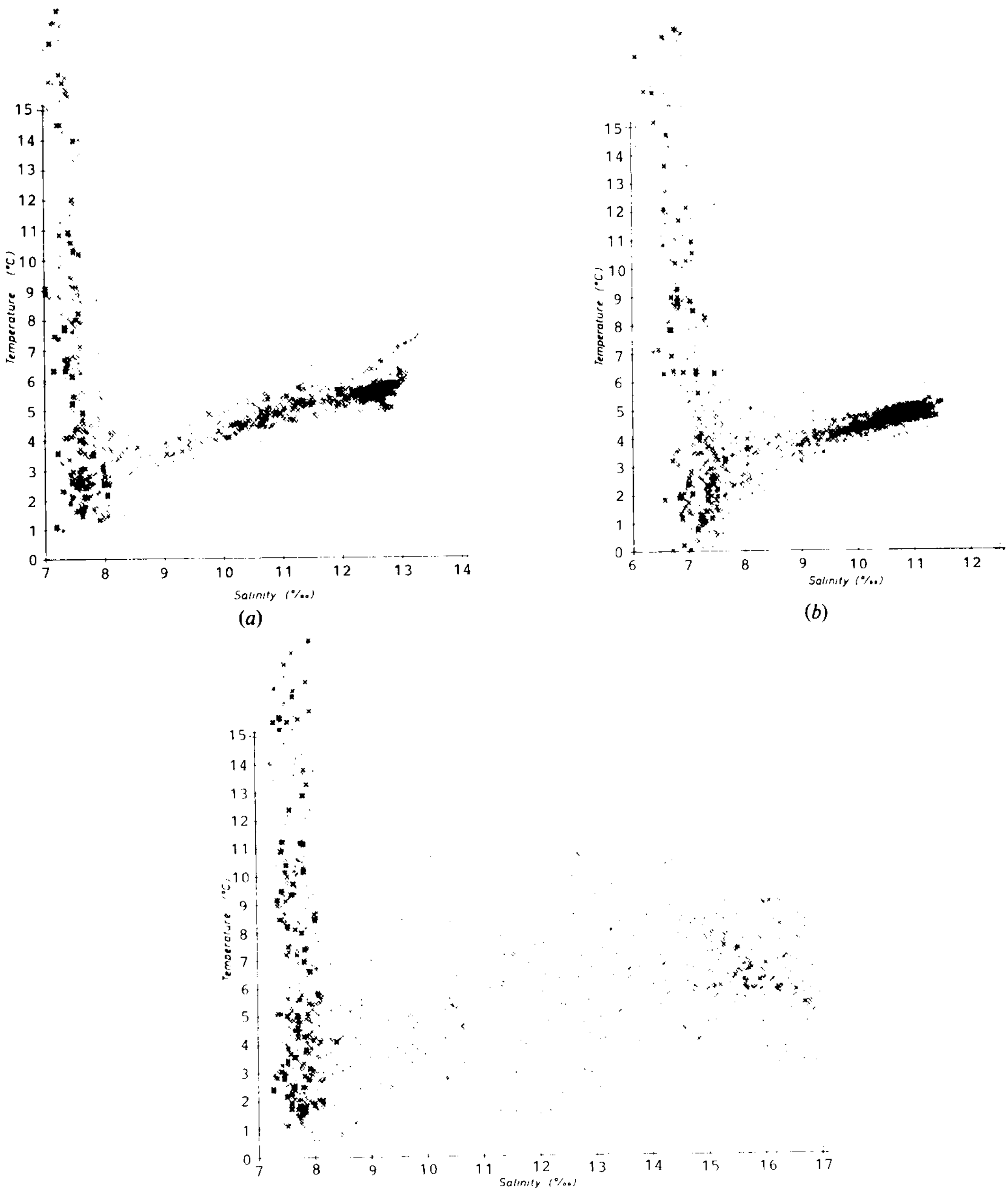

Fig. 3. T–S diagrams based on the data used in the present calculations. The diagrams are for (a) the Gotland Deep (BY15), (b) the Landsort Deep (BY31) and (c) the Bornholm Basin (BY5). An upper bound in temperature of 15 °C has been used.

Figs. 3a, b and c, where T–S diagrams from the Gotland Deep (BY15) and the Landsort Deep (BY31) are presented together with the Bornholm Basin (BY5). The relative difference in mean temperature between BY15 and BY31 is less than 0.1 °C, a value that is well below the standard errors of the two stations. The degree of scatter reflects the differences in character between the inflow region and the deeper parts of the basin. As the temperature distribution in the inflowing water, i.e. the water that flows through the Stolpe Channel is unknown, the corresponding distribution in the Bornholm Basin (BY5) is used. A consequence of this is that, to some extent, the mixing occurring in the Stolpe Channel will affect the outcome.

Hydrographic data from each station are available from routine surveys made by the Fishery Board of Sweden during the period 1963–1976, typically three to four times a year. An over-representation of certain months occurred only during the Baltic year. This bias was eliminated by only accepting one observation a month and year. The hydrographic data was then "transformed" into distributions of depth and temperature with salinity as an independent variable. Continuous mean profiles were obtained by fitting polynomials to these distributions by the least squares method. As will be evident below, the solutions are, to a large extent, qualitatively determined by the d^2T/dS^2 coefficient, since $(\gamma - T)$ is positive definite

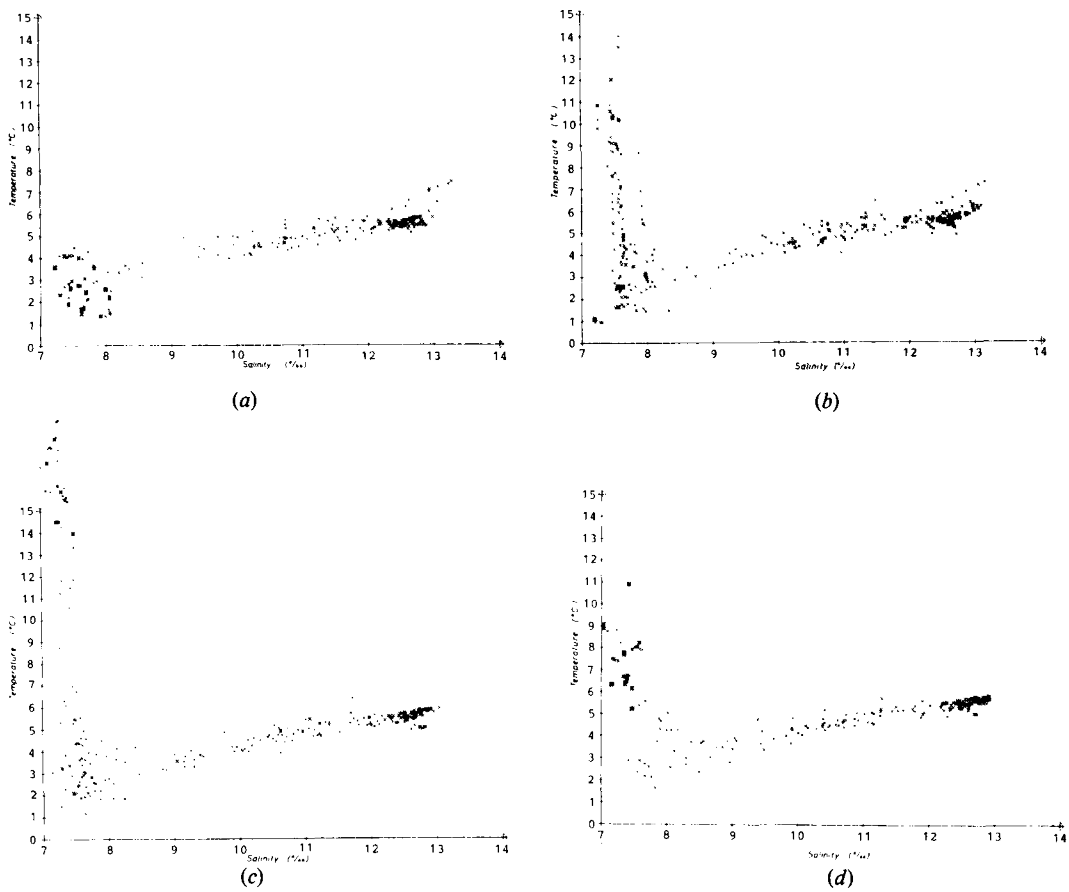

Fig. 4. T–S diagrams for the Gotland Deep based on the same data as in Fig. 3a but now separated into the different seasons of the year: (a) January–March; (b) April–June; (c) July–September; (d) October–December. An upper bound in temperature of 10 °C has been used.

and varies only slowly over the actual interval. This prompted a more thorough investigation of the hydrographic situation in the Gotland Deep. From its T–S diagram (Fig. 3a) it is evident that the main part of the profile is slightly concave, indicating (in steady-state) an upward-directed flow. However, the profile has convex end regions, implying downward-directed flows. This profile is comparable with that obtained by Alenius and Leppäranta (1982). These features are not compatible with the present view of the deep-water circulation in the Baltic, and a closer investigation reveals that these two end regions exhibit a marked seasonal variation, as is evident in Figs. 4a–d. The data in these diagrams have been arranged with respect to the quarters of the year. The bottom region is slightly warmer and saltier during springtime than during the rest of the year. This may be explained by the fact that the inflow to the Baltic is also warmer and more saline during the summer and autumn seasons than during the rest of the year. This inflow will reach the Eastern Gotland Basin half a year later, as has been reported by Fonselius (1970). Moreover, the temperature distribution in the upper region, just below the surface layer, varies with the latter. In the present work, no attempts are made to utilize this information in a time-dependent model.

3.2. *The solution*

Given the sparsity of data available, it seems reasonable to utilize polynomials of the lowest possible order. The simplest non-trivial polynomial found is of second order due to the d^2T/dS^2 coefficient. Because of the low order, these polynomials have a "smoothing" effect on the data, see Fig. 5. They are defined as

$$T = \sum_{n=0}^{2} a_n S^n, \tag{3.1a}$$

$$\gamma = \sum_{n=0}^{2} b_n S^n, \tag{3.1b}$$

and the numerical values of their coefficients are presented in Table 1.

Eq. (2.7) is, for convenience, cast into the Shrödinger form:

$$\varepsilon^2 \frac{d^2F}{dS^2} = Q(S)\cdot F, \tag{3.2}$$

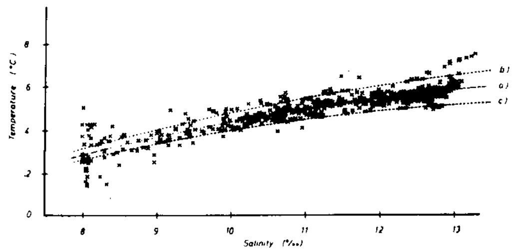

Fig. 5. T–S diagram for the Gotland Deep for salinities above 8‰. The curve (a) represents a second-order polynomial fitted to the T–S data by the least-square method. This polynomial has been perturbed by a ±8‰ change in its "highest-order" coefficient and the results are shown by the curves (b) and (c).

Table 1. *Coefficient values for the two series (3.1, a,b) based on data with a sa[illegible] above 8.0‰*

$a_0 = -7.38373184$	$b_0 = -8.02218151$
$a_1 = 1.70434475$	$b_1 = 1.90310764$
$a_2 = -0.0531878807$	$b_2 = -0.0600066185$

$$Q(S) = -\frac{d^2T}{dS^2}\bigg/(\gamma - T) = \frac{-2b_2(a_2-b_2)}{\{(a_0-b_0)+(a_1-b_1)S+(a_2-b_2)S^2\}}, \tag{3.3a}$$

$$\varepsilon^2 = (a_2 - b_2). \tag{3.3b}$$

The coefficient $Q(S)$ is positive definite over the interval. A global approximation of the solution is readily obtained by the use of the WKB method. An exponential power series of the form

$$F(S) \sim \exp\left\{\frac{1}{\delta}\sum_{n=0}^{\infty} \delta^n Y_n(S)\right\} \tag{3.4}$$

is substituted into (3.2). The first two equations become

$$\frac{d^2Y_0}{dS^2} = Q(S), \tag{3.5a}$$

$$2\frac{dY_0}{dS}\cdot\frac{dY_1}{dS} + \frac{d^2Y_0}{dS^2} = 0. \tag{3.5b}$$

The first two terms in the WKB series represent the so-called approximation of physical optics. The approximative solution, which differs from the exact solution by terms of order ε, becomes

$$F(S) \approx C_1 Q^{-1/4}(S) \exp\left\{\frac{1}{\varepsilon}\int_{S_0}^{S} Q^{1/2}(\xi)\,d\xi\right\} + C_2 Q^{-1/4}(S) \exp\left\{\frac{-1}{\varepsilon}\int_{S_0}^{S} Q^{-1/2}(\xi)\,d\xi\right\}, \quad (3.6)$$

where

$$\int_{S_0}^{S} Q^{1/2}(\xi)\,d\xi = (-2b_2)^{1/2}\left\{\arcsin\left(\frac{\alpha_1+\alpha_2-2S_0}{|\alpha_1-\alpha_2|}\right) - \arcsin\left(\frac{\alpha_1+\alpha_2-2S}{|\alpha_1-\alpha_2|}\right)\right\}, \quad (3.7a)$$

$$\alpha_{\frac{1}{2}} = -\frac{(a_1-b_1)}{2(a_2-b_2)} \pm \left(\frac{(a_1-b_1)^2}{4(a_2-b_2)^2} - \frac{(a_0-b_0)}{(a_2-b_2)}\right)^{1/2}. \quad (3.7b)$$

The coefficients C_1 and C_2 are determined by the boundary conditions (2.8) and (2.12):

$$C_1 = \frac{-F(S_0)\,Q^{1/4}(S_0)\exp\{-\varepsilon^{-1}\int_{S_0}^{S_{\max}} Q^{1/2}(\xi)\,d\xi\}}{\exp\{\varepsilon^{-1}\int_{S_0}^{S_{\max}} Q^{1/2}(\xi)\,d\xi\} - \exp\{-\varepsilon^{-1}\int_{S_0}^{S_{\max}} Q^{1/2}(\xi)\,d\xi\}}, \quad (3.8a)$$

$$C_2 = F(S_0)\cdot Q^{1/4}(S_0) - C_1. \quad (3.8b)$$

The solution (3.6) is shown graphically in Fig. 6. The supply per unit length of the salinity interval becomes, according to eqs. (2.3), (2.6) and (2.7),

$$m(S) = \frac{d^2F}{dS^2} = \frac{1}{\varepsilon^2}\,Q(S)\cdot F(S). \quad (3.9)$$

The cumulative inflow $M(S)$ is derived from (3.6) (by utilizing (2.6)),

$$M(S) = -\frac{dF}{dS} = \left\{\frac{Q^{-3/4}(S)}{4} - Q^{1/4}(S)\right\} C_1 \exp \times \{\varepsilon^{-1}\int_{S_0}^{S_{\max}} Q^{1/2}(\xi)\,d\xi\} + \left\{\frac{Q^{-3/4}(S)}{4} + Q^{1/4}(S)\right\} C_2 \exp \times \{-\varepsilon^{-1}\int_{S_0}^{S_{\max}} Q^{1/2}(\xi)\,d\xi\}. \quad (3.10)$$

Despite the inflow $m(S)$ decreasing monotonously with increasing salinity until it vanishes at the upper boundary of the salinity interval (see Fig. 6), a considerable part of the cumulative inflow $M(S)$ occurs in the salinity range above $S_{\max}$ (see also Fig. 6):

$$\psi = \frac{M(S_{\max})}{M(S_0)} \approx 10\%. \quad (3.11)$$

This is a consequence of the mixing that occurs in the Stolpe Channel. There is no way to determine the complete $m(S)$ function within the theory. The results obtained will be discussed in detail in Section 4.

4. Discussions and results

4.1. The boundary values

The boundary condition (2.12) is determined by the fresh-water supply to the Baltic ($14\cdot10^3\,m^3\,s^{-1}$) and the mean salinity of the brackish surface layer (7.8 ‰). The total inflow is $34\cdot10^3\,m^3\,s^{-1}$, based on the Knudsen relations. These values were presented by Pedersen (1977) for the same geographical area. This yields

$$F(S) = \begin{cases} 109.2\cdot10^3\ \text{kg s}^{-1} \text{ at } S = 7.8‰ \\ 0\quad\ \text{kg s}^{-1} \text{ at } S = 13.1‰. \end{cases} \quad (4.1)$$

Note that the use of the Knudsen relations in the derivation of condition (2.12) must be regarded as a lowest-order approximation in that these relations

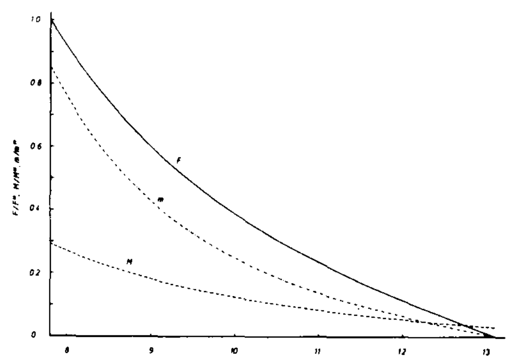

Fig. 6. Graph showing the calculated turbulent salt flux F (solid line) versus salinity. The cumulative inflow M (dashed line) and the $m(S)$ function (stippled line) are also shown. The full scale values are $F^* = 109.2\cdot10^3$ $kg\cdot s^{-1}$, $M^* = 109.2\cdot10^3\ m^3\ s^{-1}$ and $m^* = 27.3\cdot10^3$ $m^3\,s^{-1}$ per ‰.

Table 2. *Calculations of the turbulent salt fluxes F and F/A based on hydrographic data from the Gotland Deep (BY15); the estimated diffusion coefficient K is also shown*

S (‰)	dS/dz (‰ m^{-1})	z (m)	A (km^2)	$F \cdot 10^3$ (kg s^{-1})	$F/A \cdot 10^{-6}$ (kg s^{-1} m^{-2})	K (cm^2 s^{-1})	$N_{(s)}^{-1}$
8.0	0.070	61.8	70220	100.2	1.43	0.20	42
8.5	0.100	67.7	66740	81.0	1.21	0.12	36
9.5	0.087	77.6	55550	52.8	0.95	0.11	38
10.5	0.054	91.9	46120	33.2	0.72	0.13	49
11.5	0.029	120.4	27460	18.6	0.68	0.23	66
12.0	0.020	140.7	15290	12.4	0.81	0.41	80
12.5	0.006	187.9	3140	6.7	2.13	3.55	146
13.0	0.010	232.8	760	1.1	1.45	1.45	112

do not incorporate, e.g., horizontal turbulent salt fluxes, a mechanism which would lead to a decrease of the diffusive flux value. The flux values obtained by the model are presented both in Table 2 and in Fig. 6.

4.2. *The sensitivity of the model*

It is beyond the scope of this work to make a complete sensitivity analysis of the model but, by varying the polynomial for BY15 in such a way that it roughly coincides with the envelope of the T–S diagram, i.e. by varying the coefficient a_2 by ± 8%, see Fig. 5, an estimate of the probable uncertainty in $F(S)$ due to variations in T, see Fig. 7, is given. The response to $Q(S)$ is quite asymmetric. The rate of inflow, ψ, above $S = 13.1$‰ varies in this test between 8–14%.

No attempt has been made to estimate the uncertainty in γ, partly because of the basic approximation, i.e. that BY5-data are used instead of the real inflow temperatures and partly because the dominant time-scales of BY5 are probably shorter than those of BY15.

As a check on the consistency of the results, let us compare the total inflow to the basin calculated using the model and using the Knudsen relations, where the mean salinity of the inflowing water is 11 ‰ (*cf.* Pedersen, 1977). M(7.8) becomes approximately $31.9 \cdot 10^3$ m^3 s^{-1}. This value should be compared with $34 \cdot 10^3$ m^3 s^{-1}. The difference falls within the uncertainty of the approximate solution, which is of order ε, i.e., in our case ± 8%.

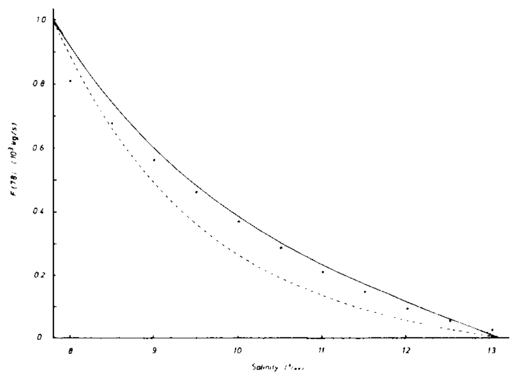

Fig. 7. Graph showing $F(S)$ (solid line) *versus* salinity. The sensitivity of the $F(S)$ solution to changes in curvature of the basin temperature profile is shown by varying the value of the coefficient a_2 by ± 8‰. The resulting solutions are shown in the graph by the dotted and stippled lines, respectively. The $F(S)$ function based on hydrographic observations in the Stolpe Channel by Rydberg (1983, personal communication) is shown by the big black dots.

4.3. *Comparisons with M(S) observations in the Stolpe Channel*

A field program, aimed at estimating the $M(S)$ function in the western part of the Stolpe Channel, has been carried out by Rydberg (1983, personal communication), though an estimate based on slightly fewer observations has been presented in Rydberg (1978). The calculated $F(S)$ distribution, based on the mean $M(S)$ function and on a no-flux condition at 14.5 ‰, is presented in Fig. 7 for the salinity interval 8–13 ‰. The agreement between this distribution and those obtained by our model is excellent, if one considers the uncertainties in both field measurements (only 9 traverse across the Stolpe Channel in 4 years) and in the determination of the boundary conditions of our model.

4.4. The F/A computations

The mean flux per unit area is also calculated; the necessary bathymetric data, such as the cross-sectional area A, is obtained from Ehlin et al. (1974) by a linear interpolation of their data and the results are presented in Table 2. The diffusive salt flux is more or less constant, $1.4\text{–}0.7 \cdot 10^{-6}$ kg $m^{-2} s^{-1}$ in the range 8–12‰, i.e. from the top of the halocline to roughly the lower part of the "Baltic intermediate water". It increases drastically below this level, hence indicating a region of more intense mixing. Further, the 12‰-isohaline coincides in the Bornholm Basin with the sill depth (60 m) of the Stolpe Channel, something that suggests the sill region as a possible region of intense mixing which is not surprising in view of the dynamics involved. The spatial resolution is, however, rather coarse due to the lowest-order approach in this single-basin model.

4.5. The vertical diffusion coefficient

A mean salt diffusion coefficient is defined in the Fickian sense by

$$\rho A K \frac{\overline{\mathrm{d}S}}{\mathrm{d}z} = F \tag{4.2}$$

where ρ and $\overline{\mathrm{d}S}/\mathrm{d}z$ are the density of the water and the mean salinity gradient, respectively. The latter is estimated for each isohaline over an interval of 0.2‰, under the assumption that the deviation of the isohaline surfaces from a horizontal surface is insignificant. These results are presented in Table 2 together with the local salinity gradient and buoyancy frequency. The dependence of the coefficient on salinity resembles that of the salt flux F/A. It is evident that the occurrence of high values of K and F/A coincides with a region in which the local salt gradient and, thus the stability, is weak. Note that this region is located below that isohaline which coincides with the sill depth of the Stolpe Channel. Low values are only obtained in the halocline and in the "intermediate water" just beneath, where the stability is strong. Estimates of this coefficient are reported from the deeper parts of the Baltic by some authors (see e.g. Matthäus, 1977; Kullenberg, 1977; Shaffer, 1979). Their values generally fall within the range 0.1–1 $cm^2 s^{-1}$ and thus are compatible with those shown in Table 2.

5. Summary

The method used (within its lowest-order concept) seems to give a reasonable estimate of the turbulent cross-isohaline salt flux of the Baltic based on the mean T–S relations of the Bornholm and Eastern Gotland Basins. The calculations are performed under two assumptions. One is that BY15 is representative for the deeper parts of the entire Baltic, something that is made probable by the high degree of lateral homogeneity observed in the T–S relations of the Baltic proper. This homogeneity does, in fact, almost preclude a multiple-basin approach. The other is that the temperature distribution at BY5 is a reasonable approximation of the inflow temperature distribution, something that is unconfirmed due to lack of pertinent data, though the governing equation is not especially sensitive to variation in γ.

The range of diffusive salt flux is determined by the boundary conditions derived by the Knudsen relations, which leaves ample scope for future improvements, but its internal distribution is given by the model as well as estimates of the $M(S)$ function with its "virtual point source" at the upper end of the salinity interval. The latter is of interest in a coming "chemical" budget of the Baltic proper.

The governing equation is rather sensitive to changes in curvature of the T–S profile in the actual basin, as is shown above. This sensitivity has focused interest on seasonal changes in the T–S relations and consequently on the seasonal variations in the in- and outflow dynamics, suggesting the use of a time-dependent version of the model in order to improve the spatio-temporal resolution and hence decreasing the sensitivity of the model to variations in curvature of T. The use of a non-conservative tracer, e.g. oxygen or phosphate, would also have this effect. Work with this purpose is already in progress, partly motivated by the need to supply a coming ecological system study of the Baltic with relevant data.

6. Acknowledgements

The author would like to thank Professor G. Walin for initiating this investigation and for his continuous support. The author also wants to express his gratitude to Mr. U. Jonasson and Mr. O. Åkerlund for valuable help with the data processing and the Institute staff for their help in preparing the manuscript.

REFERENCES

Alenius, P. and Leppäranta, M. 1982. Statistical features of hydrography in the northern Baltic Sea. Proc. 13th Conf. Baltic Oceanogr., Helsinki, 95–104.

Bolin, B. 1972. Model studies of the Baltic Sea. *Ambio Special Report 1*, 115–119.

Ehlin, U., Mattison, I. and Zachrisson, G., 1974. Computer based calculations of volume of the Baltic area. Proc. 9th Conf. Baltic Oceanogr., Kiel, 115–128.

Fonselius, S. H. 1970. On the stagnation and recent turnover of the water in the Baltic. *Tellus 22*, 533–544.

Holland, W. 1971. Ocean tracer distributions—a preliminary numerical experiment. *Tellus 23*, 371–392.

Kullenberg, G. 1977. Observation of the mixing in the Baltic thermo- and halocline layers, *Tellus 29*, 572–587.

Matthäus, W. 1977. Mittlere vertikale Wärmeaustauschkoeffizienten in der Ostsee. *Acta Hydrophys. 22*, 73–92.

Pedersen, F. B. 1977. On dense bottom currents in the Baltic deep water. *Nord. Hydrol. 8*, 297–316.

Rydberg, L. 1978. Deep water flow and oxygen consumption within the Baltic. Report No. 27, Oceanographic Institute University of Gothenburg.

Sarkisyan, A. S., Stashkevich, A. and Kowalik, Z. 1978. Diagnostic computation of the summer circulation in the Baltic Sea. *Oceanol. 15*, 653–656.

Shaffer, G. 1979. Conservation calculations in natural coordinates. *J. Phys. Oceanogr. 9*, 847–855.

Shaffer, G. and Rönner, U. 1984. Denitrification in the Baltic proper deep water. *Deep Sea Res. 31*, 197–220.

Veronis, G. 1975. The role of models in tracer studies. In: *Numerical models of ocean circulation* (ed. Reid, R. O., Robinson, A. R. and Bryan, K.). National Academy of Sciences, Washington, D.C., 349–360.

Walin, G. 1977. A theoretical framework for the description of estuaries. *Tellus 29*, 128–136.

Walin, G. 1981. On the deep-water flow into the Baltic. *Geophysica 17*, 75–93.